Supplement of The Cryosphere, 14, 2883–2908, 2020
https://doi.org/10.5194/tc-14-2883-2020-supplement

The Cryosphere
Open Access

Supplement of

Revealing the former bed of Thwaites Glacier using sea-floor bathymetry: implications for warm-water routing and bed controls on ice flow and buttressing

Kelly A. Hogan et al.

Correspondence to: Kelly A. Hogan (kelgan@bas.ac.uk)

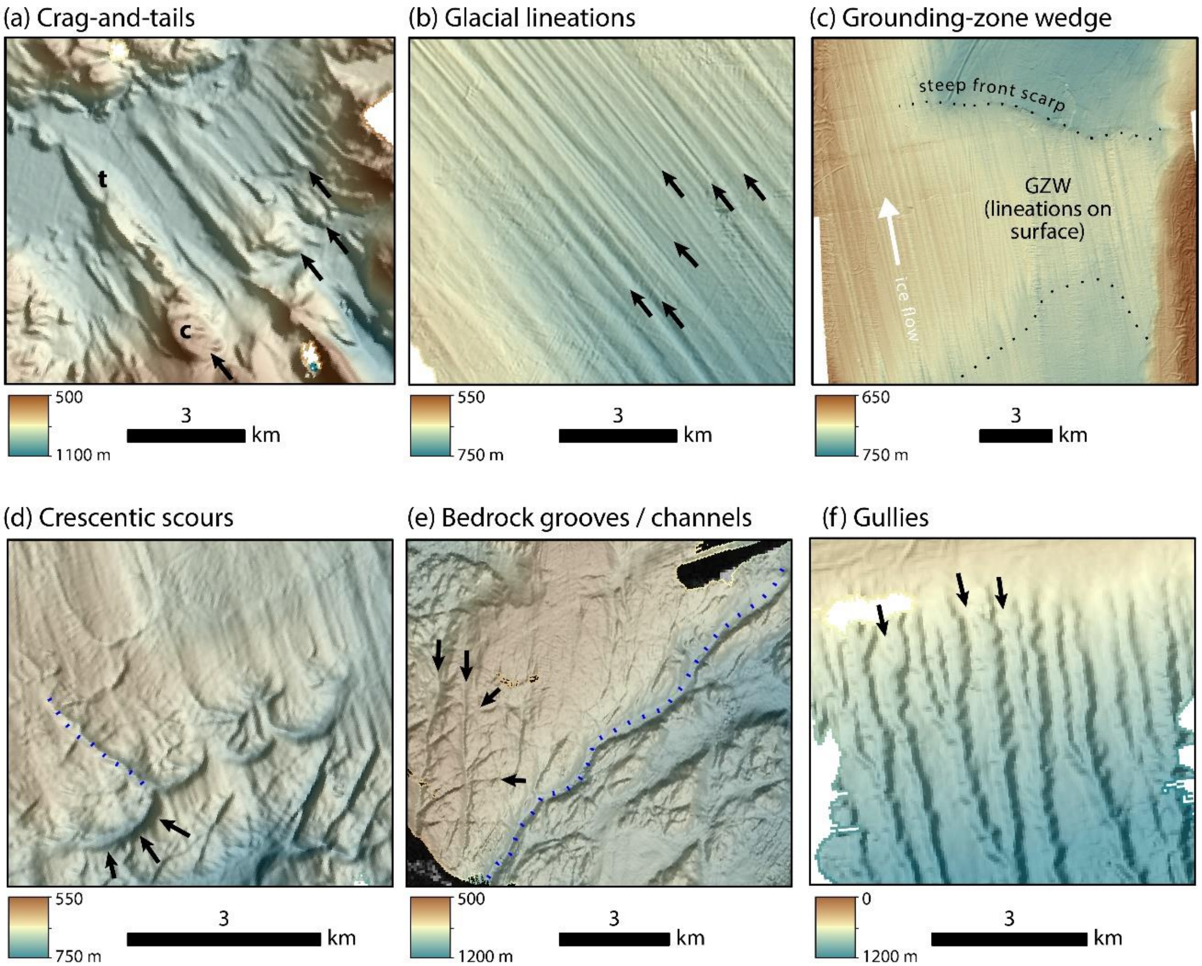

Supplementary Figure S1: Examples of glacial landforms discussed in the text; all examples are from the Amundsen Sea Embayment. (a) Crag-and-tail landforms (several arrowed) from Pine Island Bay with bedrock crags "c" and sedimentary tails "t" streamlined in the direction of ice flow. (b) Glacial lineations from the Dotzon-Getz palaeo-ice stream trough (several arrowed) and fully described in Graham et al. (2009). (c) A grounding-zone wedge (GZW) from Pine Island Trough on the outer continental shelf. The subtle asymmetric wedge rises only 20 m above the surrounding sea floor and has been overridden by ice as shown by the glacial lineations on its surface. (d) Crescentic scours (curved channels; one arrowed) on the ice-proximal side of the H3 high. Note a bedrock channel is marked by blue dots. (e) Grooves (arrowed) and a channel incised in to bedrock in front of TG. Note the linear or slightly curvilinear form of the grooves which form a crossed patterned of incision versus the sinuous, continuous form of the channel (blue dots). (f) Gullies (arrowed) – relatively straight channels incising a slope - at the shelf edge of the Amundsen Sea.

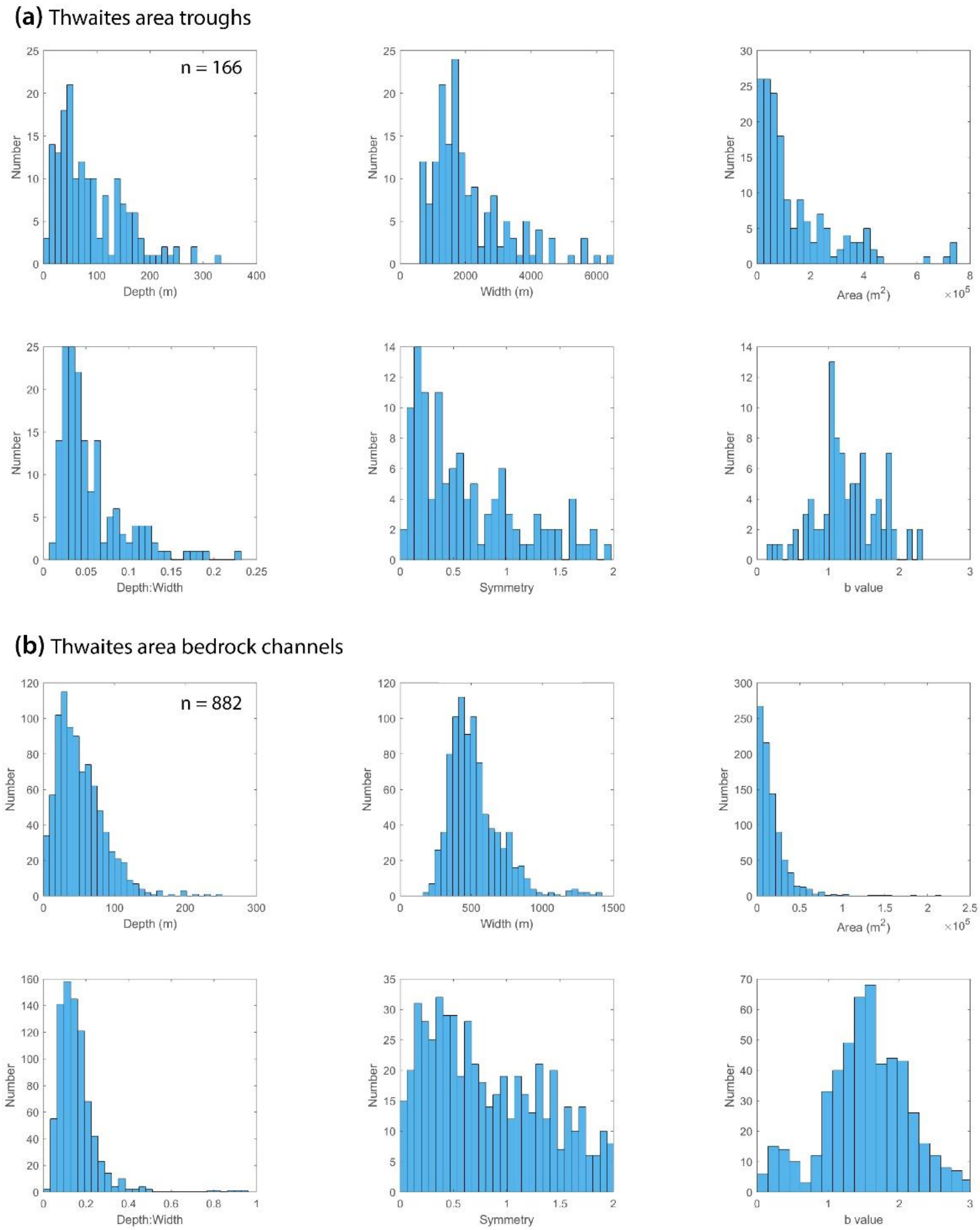

Supplementary Figure S2: Cross-sectional metrics for (a) bathymetric troughs and (b) bedrock channels identified from the MBES dataset in front of Thwaites Glacier (troughs and channels are mapped in Fig. 3). Note the different scales on some axes. Symmetry values of 1 denote perfectly symmetrical cross sections whilst values >1 and <1 denote left-skewed and right-skewed cross sections, respectively. The b value assesses how V- or U-shaped a cross section is; values of 1 are perfectly V shaped, values of 2 are perfectly U shaped. b values greater than 2 reflect box shaped geometries and values below 1 indicate convex-upward forms.

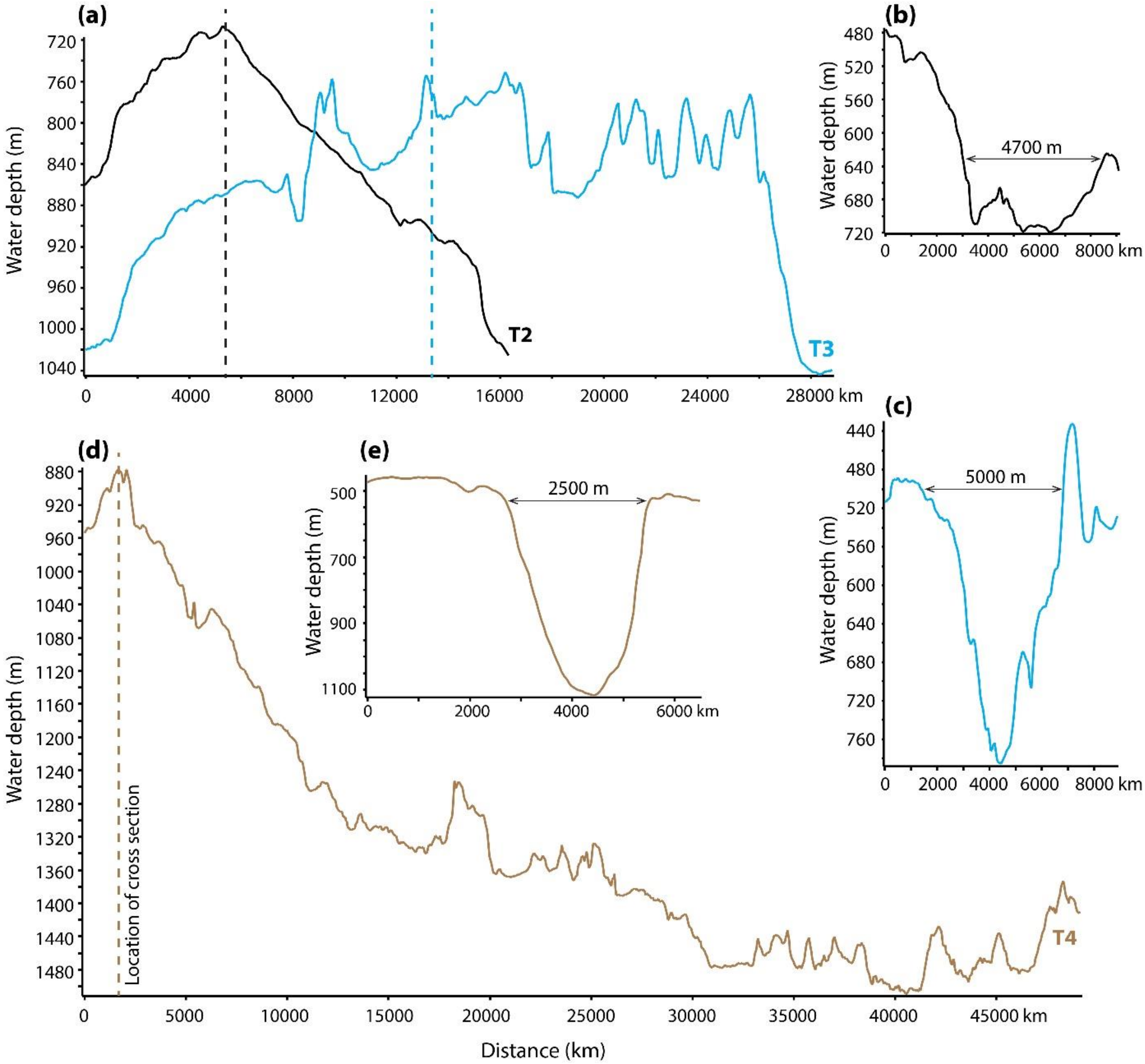

Supplementary Figure S3: Long profiles and cross-sections for sea-floor troughs in front of Thwaites Glacier. (a) Long profiles for T2 and T3 troughs showing locations of bathymetric sills. (b) Cross section over sill in T2 trough (located in (a)). (c) Cross section over sill in T3 trough (location in (a)). (d) Long profile for T4 trough. (e) Cross section over sill in T4 trough (located in (a)). See Fig. 3a in the main text for locations of long profiles in (a) and (d).

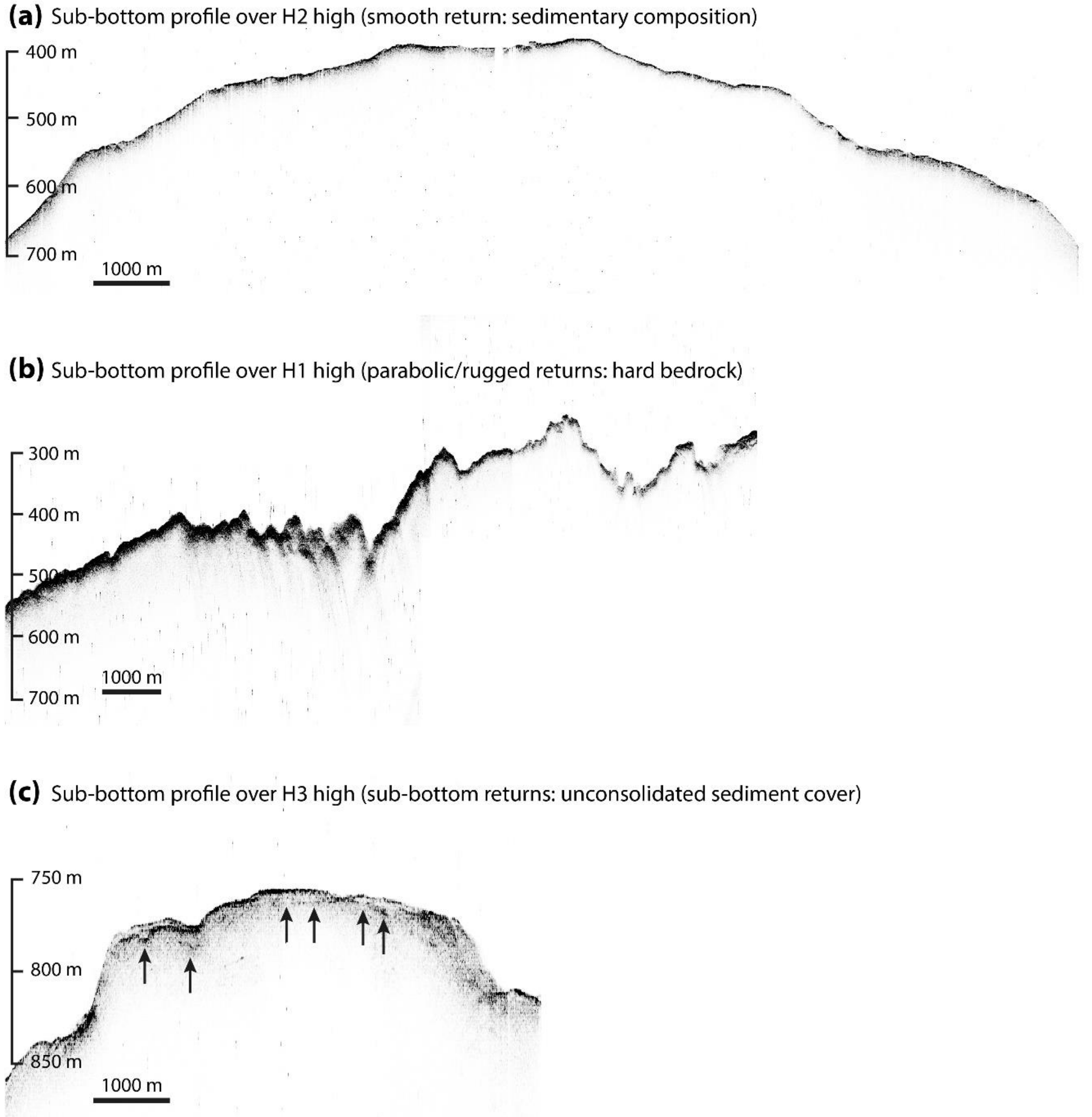

Figure S4: Example of Knudsen Chirp sub-bottom profiles over the sea-floor highs north of Thwaites Ice Shelf. (a) is a profile over the H2 high showing a very smooth return interpreted as sediment cover that is co-located sedimentary landforms (GZW) observed on MBES data. (b) is a profile from the flank of the H1 high showing diffraction parabola from point reflectors at the sea floor interpreted as hard bedrock lithology. (c) is a profile from the H3 high showing up to 15 m of unconsolidated sediment cover; sub-sea-floor reflections are marked by arrows. All profiles were acquired during cruise NBP19-02 (Larter et al., 2020).

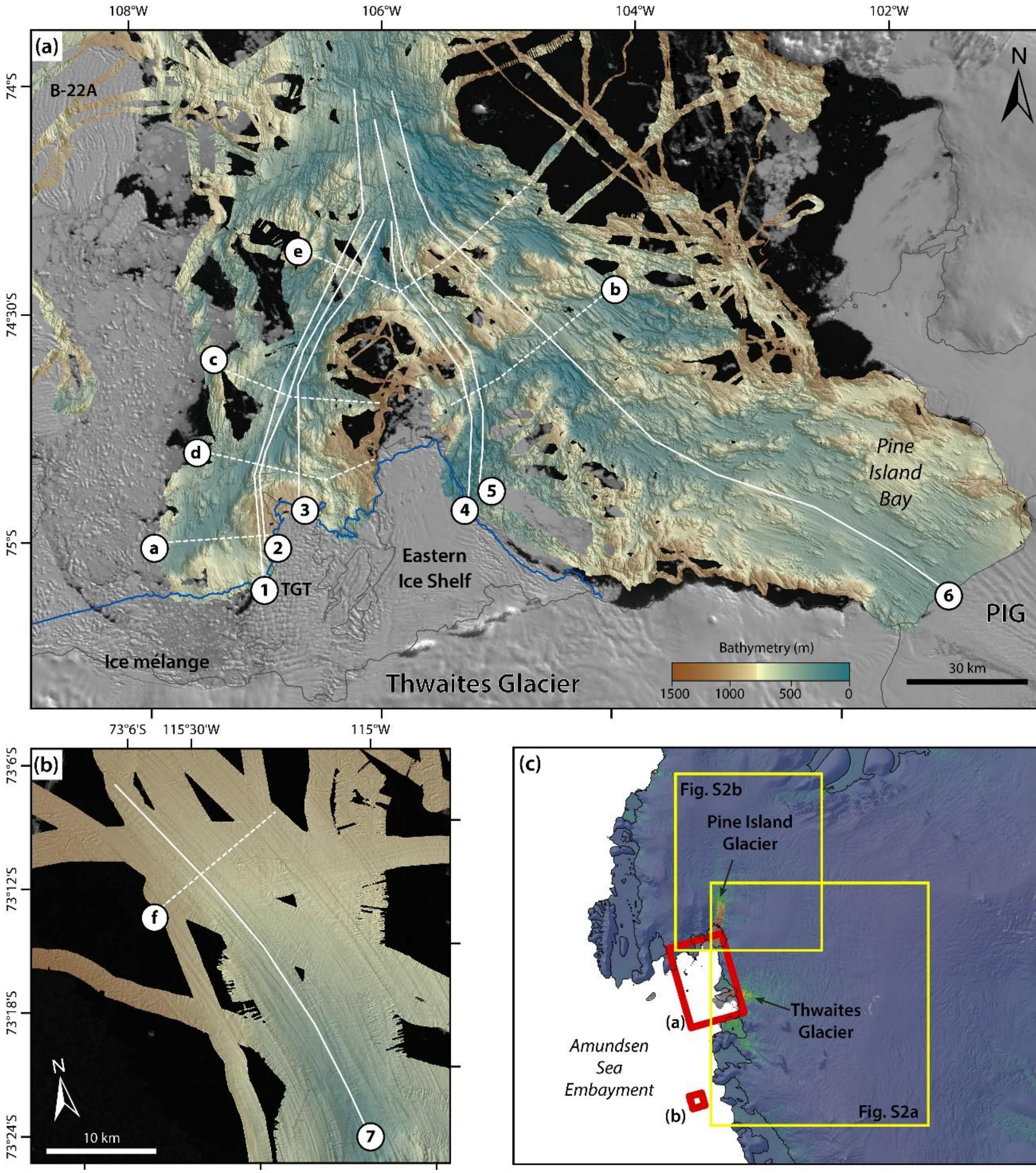

Supplementary Figure S5: Location maps for bed profiles used in roughness and drag contribution analyses (see Sections 2.2 and 4 in the main text). (a) Palaeo-glacier bed profiles from MBES data offshore Pine Island and Thwaites glaciers. Along-flow profiles are labelled (1)-(6); across-flow profiles are labelled (a)-(e). (b) Palaeo-glacier bed profiles for a "smooth" bed characterised by mega-scale glacial lineations (MSGL) in the mid-shelf section of Dotson-Getz Trough; along-flow profile is labelled (7), across-flow profile is labelled (f). (c) Location map of the Amundsen Sea Embayment and the Amundsen Sea sector of the West Antarctic Ice Sheet showing the locations of Supplementary Figures S1a, b (red outlines) and S2a, b (yellow outlines).

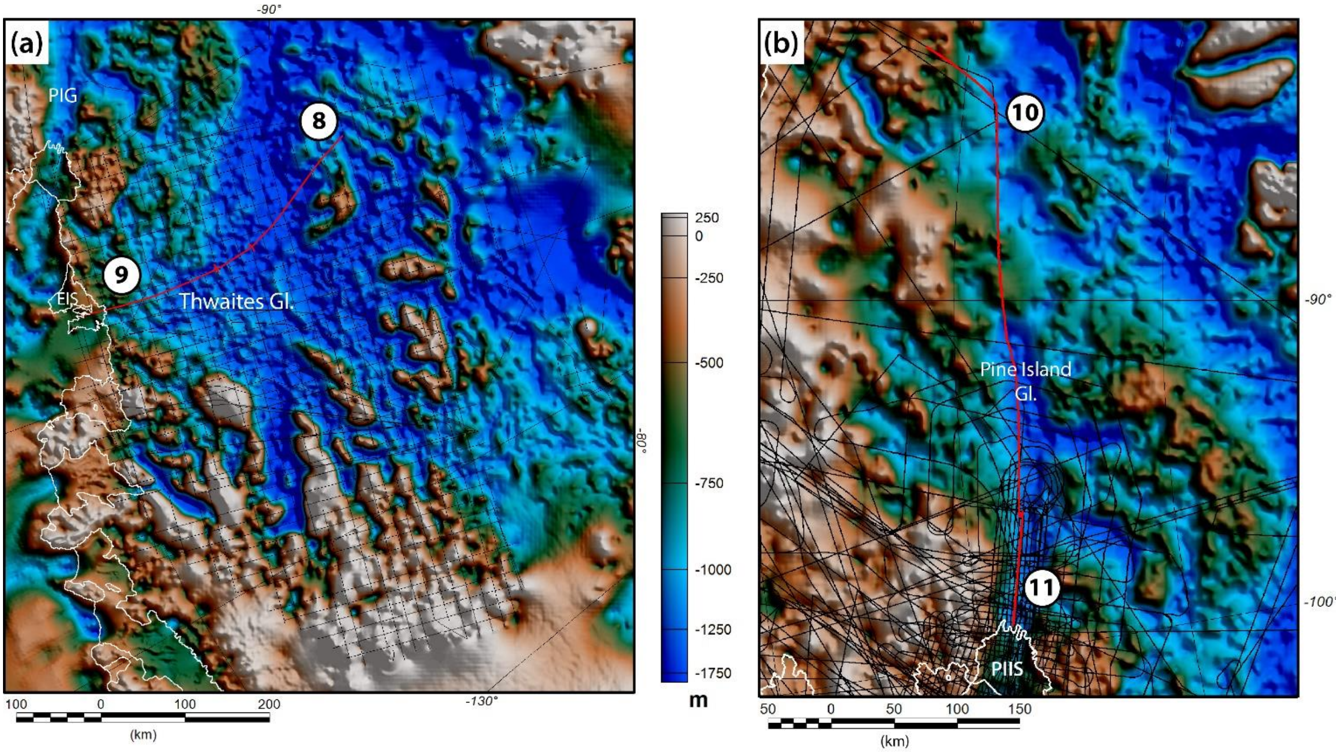

Supplementary Figure S6: Location maps for airborne radar (onshore) bed profiles used in roughness and drag contribution analyses. (a) AGASEA line used for modern Thwaites Glacier bed profiles; the tick marks denote the ends of the two profiles shown in Fig. S4f and S4g; note the overlap between the profiles. PIG is Pine Island Glacier; EIS is the Eastern Ice Shelf of Thwaites Glacier. (b) OIB profile for modern Pine Island Glacier bed profiles. PIIS is Pine Island Ice Shelf.

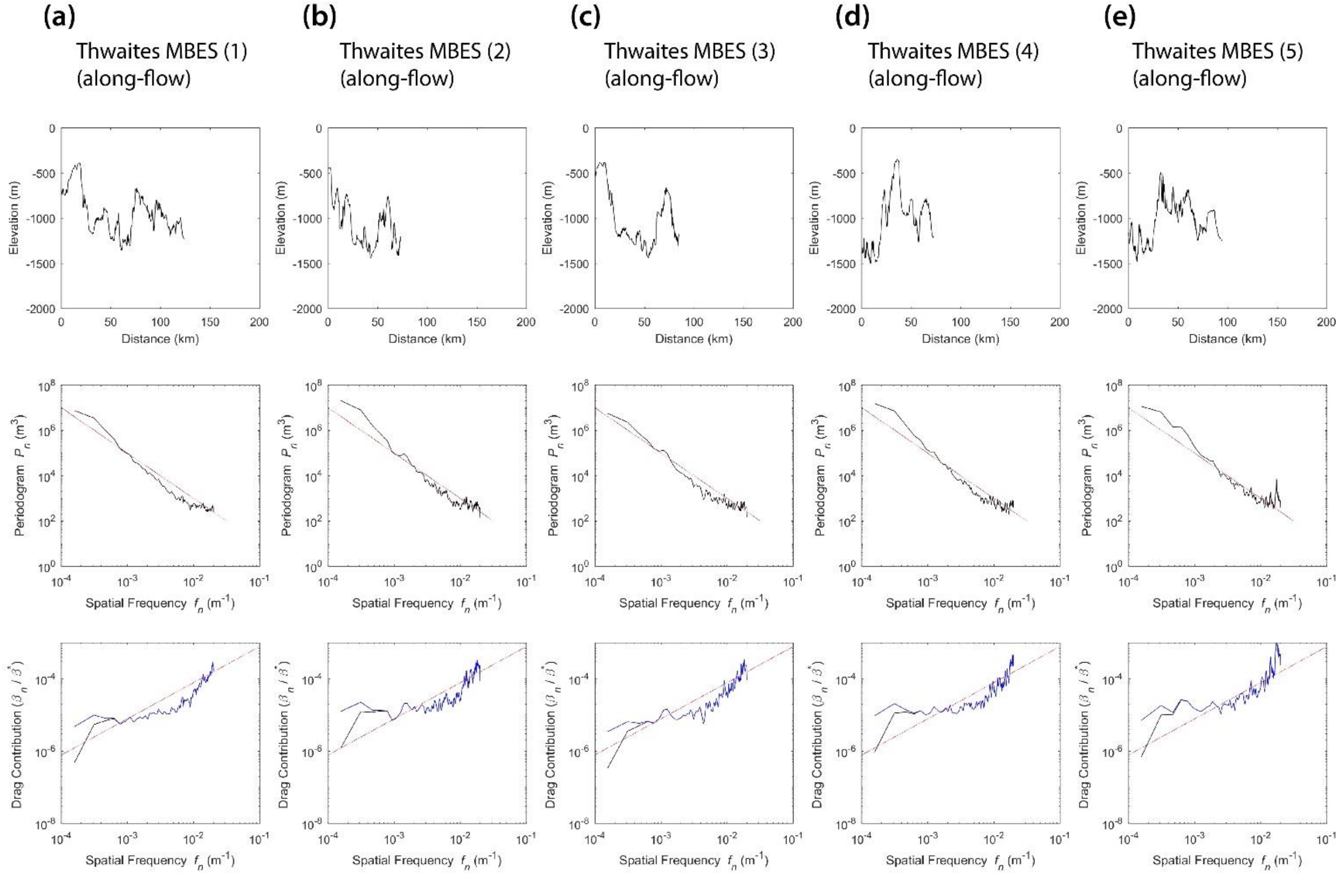

Supplementary Figure S7: Bed profiles (top), derived power spectra (middle) and basal drag contributions (bottom) for all bed profiles used in this study, for locations see Figs. SF1 and SF2: (a) Thwaites MBES along-flow profile 1; (b) Thwaites MBES along-flow profile 2; (c) Thwaites MBES along-flow profile 3; (d) Thwaites MBES along-flow profile 4; (e) Thwaites MBES along-flow profile 5. As per the main text (Section 4, Figs, 6, 7), the red line in power spectra and drag contribution plots are based on an assumption of Brownian motion (i.e. power decays as inverse square of spatial frequency). At low spatial frequency, drag contributions depend on the function *F*. Two limiting cases are shown: F_1 (blue), F_2 (black).

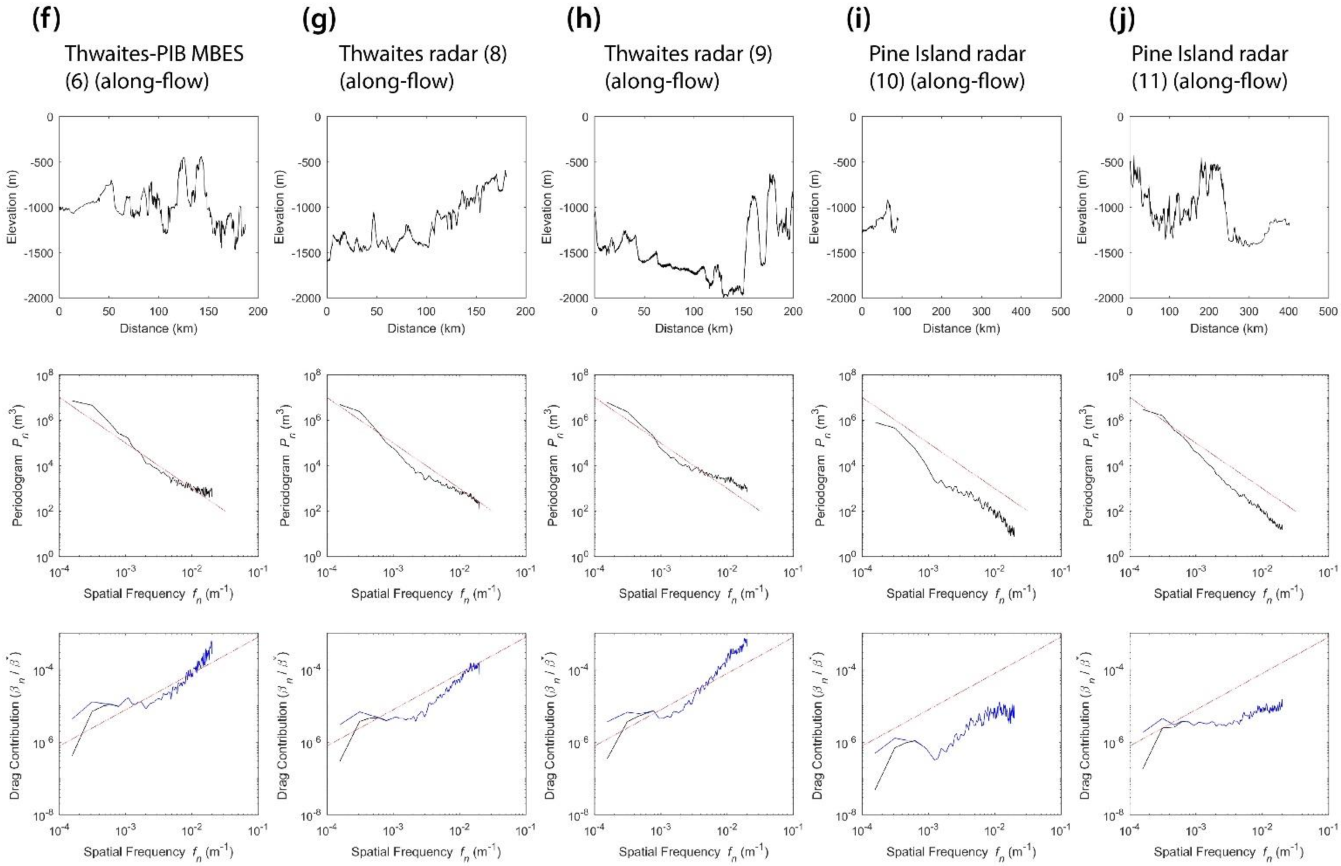

Supplementary Figure S7 (continued): Bed profiles (top), derived power spectra (middle) and basal drag contributions (bottom) for bed profiles used in this study, for locations see Figs. SF1 and SF2: (f) Thwaites-Pine Island MBES along-flow profile 6; (g) Thwaites radar along-flow profile 8 (upstream area); (h) Thwaites radar along-flow profile 9 (downstream area); (i) Pine Island radar along-flow profile 10 (upstream area); (j) Pine Island radar along-flow profile 11 (downstream area).

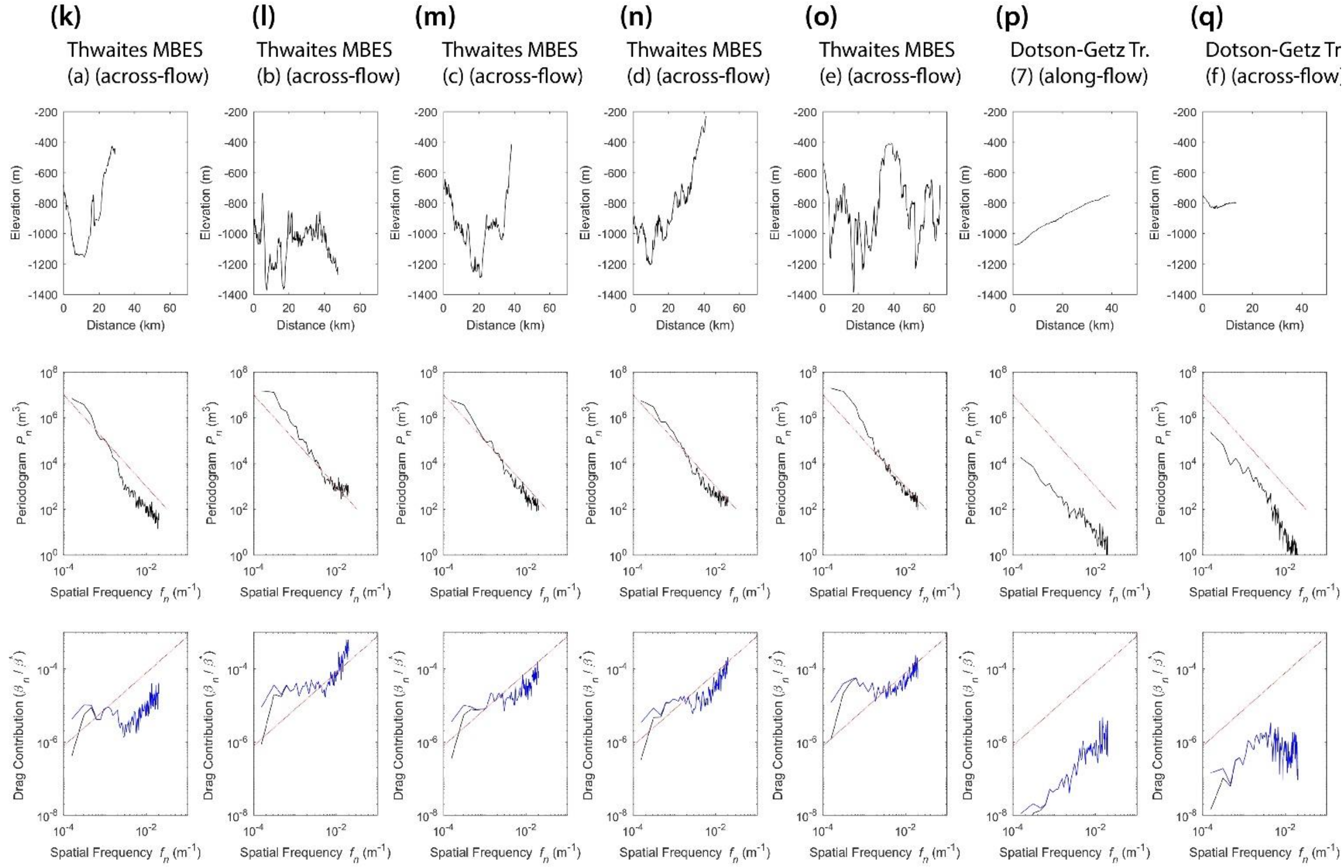

Supplementary Figure S7 (continued): Bed profiles (top), derived power spectra (middle) and basal drag contributions (bottom) for bed profiles used in this study, for locations see Figs. SF1 and SF2: (k) to (o) are Thwaites MBES across-flow profiles a-e, respectively; (p) is the Dotson-Getz Trough along-flow profile (7); (q) Dotson-Getz Trough across-flow profile f.

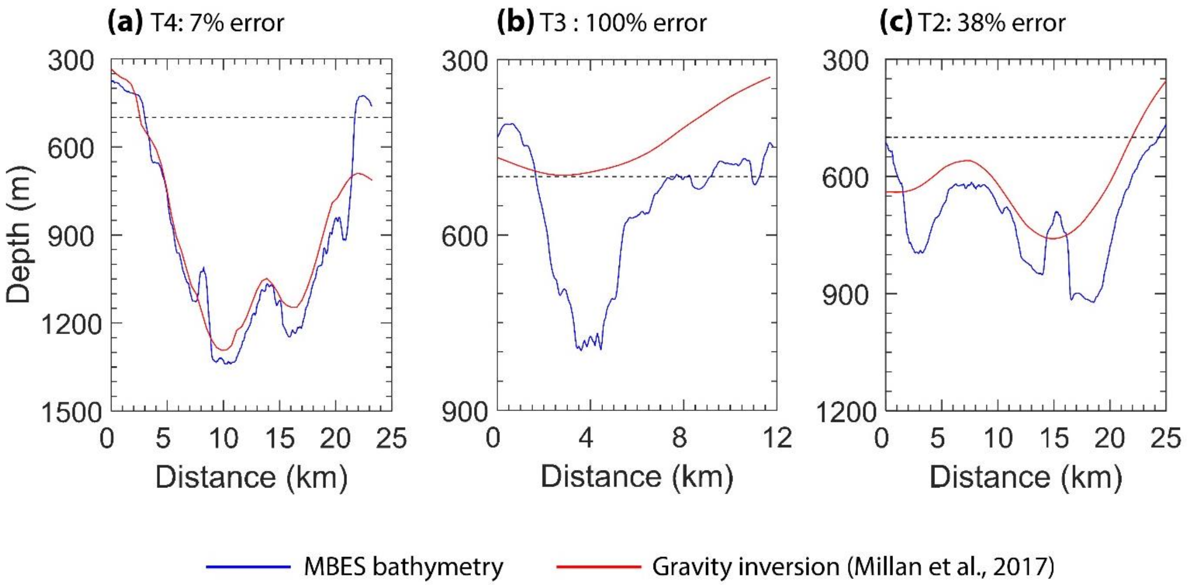

Supplementary Figure S8: Comparisons of cross-sections over troughs that act as pathways for CDW to the Thwaites grounding zone from our MBES data (blue) and Millan et al. (2017) (red). Locations of the troughs are marked by asterisks in Fig. 8a. For trough T4 east of the EIS (a) the gravity-inversion only gives a 7% error in the trough cross-sectional area compared with the MBES grid below 500 m (dashed line). Trough T3 between the H1 and H2 highs (b) is not resolved by Millan et al. (2017), i.e. the error is 100% below 500 m. The rugged sea floor of trough T2 (c) is poorly-resolved by the Millan et al. (2017) grid resulting in a 38% error in cross-sectional area.

The table below gives the area of any parts of the cross section that are below 500 m depth.

Trough	NBP19-02 area (km^2)	Millan area (km^2)	Area difference (%)	'Missing water' (km^2)
T4	10.3	9.78	4.72*	0.52
T2	0.88	0	100	0.88
T3	5.17	3.20	38.1	1.97

Supplementary Table 1: Cross-sectional area difference calculations for Millan et al. (2017) and the MBES grid for three troughs (locations are given as asterisks in Fig. 8a). Trough cross-sectional areas are calculated using trapezoidal numerical integration for any part of the trough below 500 m; the depth below which CDW is assumed to be present. *The channel area difference for T4 increases to 7% if we ignore the part of the cross-section from 22 km onwards, which in the Millan et al. (2017) grid underestimates the flank of the channel.

Oceanic heat flux calculations

To estimate the heat fluxes through troughs defined by the new MBES grid and the existing regional bathymetric grid of Millan et al. (2017) (Sect. 6.1) we use the equation for heat flux (W/m^2) per unit area as given by (Arneborg et al., 2012):

$$F = \rho C_P U (T - T_F) \qquad \text{(eqn. 1)}$$

Where ρ (kg m^{-3}) is the water density, C_P (J kg^{-1} K^{-1}) is the specific heat capacity, U (m s^{-1}) is the velocity in the along-trough direction, T (K) is temperature, and T_F (K) is the freezing temperature. The total heat flux H (TW) is then obtained by integrating the flux over a cross-section of the trough. We perform the calculations for trough T2 which showed a 38% increase in cross-sectional area between the regional and MBES bathymetries (see Supp. Table 1). To match these areas we use trough depths as defined by the regional bathymetry (750 m) and our MBES data (900 m), and use a simplified geometry with a constant width below 500 m calculated to match the cross-sectional areas. For example, to obtain a cross-sectional area of 5.2 km^2 (below 500 m) we use a trough width of 13 km, that is 5.2 km^2 divided by 900 m minus 500 m.

For the calculations, we also need a suitable temperature profile for the water masses in the troughs and the water velocity through the troughs. Recent studies have shown that ocean temperature increases as a function of depth on the inner Amundsen Sea shelf (Christianson et al., 2016; Webber et al., 2019), and that velocity increases with depth approximately proportionally to temperature (Arneborg et al., 2012; Wåhlin et al., 2020). The proportionality occurs because the bottom-intensified component of velocity is driven by the density difference between the deep current and the ambient water, which in these waters is a function of temperature. It has also been shown that the density-driven component, in contrast to the vertically constant (wind-driven) component, is more likely to make it to the grounding zone whereas the wind-driven component can be blocked at the ice shelf front (Wåhlin et al., 2020). Thus, we assume a linear increase in temperature from freezing point at 300 m to pure Circumpolar Deep Water (1.2 ºC) at 800 m, similar to observations in Pine Island Bay (Christianson et al., 2016), as well as further west (Arneborg et al., 2012). We perform the calculations for both a constant along-trough velocity (U) and also for a velocity that is proportional to temperature according to (Arneborg et al., 2012):

$$U = 0.02 + 0.01T \qquad \text{(eqn. 2)}$$

This takes into account the velocity dependence on density and resembles average velocity profiles in the western Amundsen Sea Embayment (Arneborg et al, 2012).

The table below gives the estimated total heat flux through trough T2 with the different parameters as discussed above.

T2 trough depth (m)	Bathymetric source	Velocity profile	Total heat flux, H (TW)
750	Millan et al. (2017)	Constant	0.5
900	MBES (this study)	Constant	1.11
750	Millan et al. (2017)	Proportional to T	0.45
900	MBES (this study)	Proportional to T	1.27

Supplementary Table 2: Total heat flux estimates through T2 using trough cross-sectional areas as defined by Millan et al. (2017) and the MBES grid (this study).

References

Arneborg, L., Wåhlin, A., Björk, G., Liljebladh, B., and Orsi, A.: Persistent inflow of warm water through a submarine trough on the Western Amundsen Shelf. Nature Geoscience, 5, 876-880, 2012.

Christianson, K., Bushuk, M., Dutrieux, P., Parizek, B. R., Joughin, I. R., Alley, R. B., Shean, D. E., Abrahamsen, E. P., Anandakrishnan, S., Heywood, K. J., Kim, T. W., Lee, S. H., Nicholls, K., Stanton, T., Truffer, M., Webber, B. G. M., Jenkins, A., Jacobs, S., Bindschadler, R., and Holland, D. M.: Sensitivity of Pine Island Glacier to observed ocean forcing, Geophysical Research Letters, 43, 10817-10825, doi:10.1002/2016GL070500, 2016.

Graham, A. G. C., Larter, R. D., Gohl, K., Hillenbrand, C.-D., Smith, J. A., and Kuhn, G.: Bedform signature of a West Antarctic palaeo-ice stream reveals a multi-temporal record of flow and substrate control, Quaternary Science Reviews, 28, 2774-2793, 2009.

Wåhlin, A. K., Steiger, N., Darelius, E., Assmann, K. M., Glessmer, M. S., Ha, H. K., Herraiz-Borreguero, L., Heuzé, C., Jenkins, A., Kim, T. W., Mazur, A. K., Sommeria, J., and Viboud, S.: Ice front blocking of ocean heat transport to an Antarctic ice shelf, Nature, 578, 568-571, 2020.

Webber, B. G. M., Heywood, K. J., Stevens, D. P., and Assmann, K. M.: The Impact of Overturning and Horizontal Circulation in Pine Island Trough on Ice Shelf Melt in the Eastern Amundsen Sea, Journal of Physical Oceanography, 49, 63-83, 2019.